minerals

MDPI

Article

A Solid State NMR Investigation of Recent Marine Siliceous Sponge Spicules

Sylvie Masse [1,*,†], Andrzej Pisera [2,†], Guillaume Laurent [1] and Thibaud Coradin [1]

[1] Sorbonne Universités, UPMC Univ Paris 06, CNRS, Collège de France, Laboratoire de Chimie de la Matière Condensée de Paris (LCMCP-UMR 7574), 11 place Marcelin Berthelot, F-75005 Paris, France; guillaume.laurent@upmc.fr (G.L.); thibaud.coradin@upmc.fr (T.C.)

[2] Institute of Paleobiology, Polish Academy of Sciences, ul. Twarda 51/55, 00-818 Warszawa, Poland; apis@twarda.pan.pl

* Correspondence: sylvie.masse@upmc.fr; Tel.: +33-1-4427-1527

† These authors contributed equally to this work.

Academic Editor: Caroline Peacock

Received: 18 December 2015; Accepted: 26 February 2016; Published: 10 March 2016

Abstract: The composition of four recent siliceous marine sponge spicules was studied and compared. In particular, multinuclear (^{29}Si, ^{13}C, ^{31}P) solid state nuclear magnetic resonance (NMR) allowed the characterization of both the mineral and organic constituents in a non-destructive manner. The silica network condensation was similar for all samples. The organic matter showed a similar pattern but varied in abundance as a function of the sponge group (Hexactinellida or Demospongiae) and sampling conditions (living or dead organisms). This indicates that the striking morphological differences observed at the macroscale for the various samples do not lead to significant fingerprints in the spectroscopic signatures of the mineral and organic constituents.

Keywords: sponges; silica; solid state nuclear magnetic resonance (NMR)

1. Introduction

Nature offers a great variety of beautiful examples of biomineral materials [1]. In the marine world, diatoms, which are planktonic unicellular algae, and siliceous sponges represent striking examples of mineralized living organisms [2]. The complexity encountered in their composition and the beauty of their structure make them model systems for studying natural bioorganic/inorganic hybrid materials in order to improve our knowledge of the interactions between silica and organic matter [3]. In such systems, natural silica—we can call "biogenic silica" because it is completely generated by living cells themselves—which represents a production of 10^{10} tons per year lying in ocean depths, is in perpetual interaction with the surrounding organic and biological environment [4].

Sponges are the only Metazoans using silicon on a large scale to build their skeleton [5]. The skeleton shape and organization is species-specific and therefore under genetic control. Among the phylum Porifera, more than 90% of the 8716 species of sponges belong to the group of Demospongiae, living in marine and (a small fraction) in freshwater, from shallow to deep waters, and looking like soft, tough, and often brightly colored species. Because of their great variety of shapes, sizes and textures, this class is known as the most varied class of siliceous sponges. On the contrary, hexactinellids (also referred to as "glass sponges") are relatively uncommon and are mostly encountered at sea depths of hundreds of meters and more. The siliceous spicules of most hexactinellids, which are usually made of six rays, are larger and form skeletons more luxuriously architectured than those in demosponges [6]. Among siliceous sponges, two types of spicules exist: the microscleres and the megascleres [7]. Whereas microscleres are of small size (1–100 μm) and are not implicated in the skeletal structure, megascleres, which are larger (from 100 μm up to 3 m long, in the case of the giant

spicule of Hexactinellida), contribute actively to supporting tissues and can serve at the anchoring in the mud.

An outstanding feature of siliceous spicules, from both Demospongiae and Hexactinellida, is the formation of the silica shell around an axial filament. The major protein of the axial filament of the demosponge *Tethya aurantium* is an enzyme termed as *silicatein* by Morse *et al.*, which mediates polymerization/condensation of orthosilicate to polymeric (bio)silicate [8]. In their study on *Monorhaphis chuni* and *Monorhaphis intermedia* (hexactinellids), Müller *et al.*, proposed that the growth of spicules starts intracellularly and proceeds by lamellar apposition of silica layers, separated by sheets of organic matrices formed by a very likely silicatein-like protein(s) and a lectin [9]. The outer surface of the spicules would be covered by a collagen net. However, despite the attractiveness of biosilica for biotechnological applications [10] and despite the fact that only sponges produce enzyme-mediated silica, only a few detailed analyses of the proteinaceous components of spicules from hexactinellids exist [11].

From a materials perspective, biominerals are considered as hybrid or nanocomposite organic-inorganic systems [12]. Hence, a wide range of spectroscopic techniques initially developed for the characterization of synthetic solids belonging to this class of materials has been applied over the last years to natural phases [13–16]. In particular, solid state nuclear magnetic resonance (NMR) is a powerful tool as it is a non-destructive method allowing for the parallel study of mineral and organic components, as well as of their interface, via cross-polarization and two-dimensional (2D) methods [17]. In the case of silica, it is possible to link the ^{29}Si chemical shift with the coordination sphere of the silicon atom and therefore to characterize the condensation state of the mineral phase. On this basis, biogenic silica from diatoms [18,19] and plants [20] has been studied by ^{29}Si and, in some cases, by ^{1}H, ^{13}C and ^{15}N NMR. Here we were interested in applying this technique to recent sponges belonging to different groups in order to identify possible species-specific spectroscopic signatures.

2. Results

2.1. Sample Presentation and General Characterization

In this study, four recent (within the meaning of the paleontologists/geologists, that is to say Holocene-aged) sponge spicule samples were investigated. They belong to the phylum Porifera and represent two different classes, Demospongiae and Hexactinellida. "Soft" demosponges (that have no articulated spicules) Petrosidae (PETRO) and *Geodia* (GEODIA) were chosen as representative for this group. The group of hexactinellids was represented by exploring *Aphrocallistes* (APHRO) and *Laocoetis perion* (also known as *Craticularia)* (LAOCO) samples. APHRO and PETRO samples were collected alive whereas GEODIA and LAOCO were collected dead and stored for a long period (>30 years).

The samples were examined by scanning electron microscopy (SEM) (Figure 1). For PETRO, Figure 1a shows the cross-section of the raw material that appears as discrete siliceous spicules bound together by a matrix known to be composed only of organics. After removal of the organic component by acidic treatment, loose spicules of various morphology (mostly simple spicules called oxeas) and size that occur in the sponge body are observed (Figure 1b). For GEODIA, the cross-section of the sponge shows siliceous spicules embedded into the organic matrix (Figure 1c). After acidic cleaning, one should note the thick external layer of spherical spicules, with star-like ornamentation, called sterrasters (details shown in Figure 1d), that are characteristic for this sponge. In APHRO, the internal natural surface view shows the characteristic honey-comb structure of the skeleton composed of fused-together (in opposition to demosponges where spicules are only bound by organics) siliceous spicules called hexactines (Figure 1e). Figure 1f shows the details of the skeleton after acidic treatment. LAOCO is characterized by an upper surface of the skeleton composed, after acidic treatment, of fused, strongly silicified and modified hexactines, with regularly organized canal openings (Figure 1g). Details of the lower surface revealing strongly modified, ornamented and fused hexactine spicules are shown in Figure 1h.

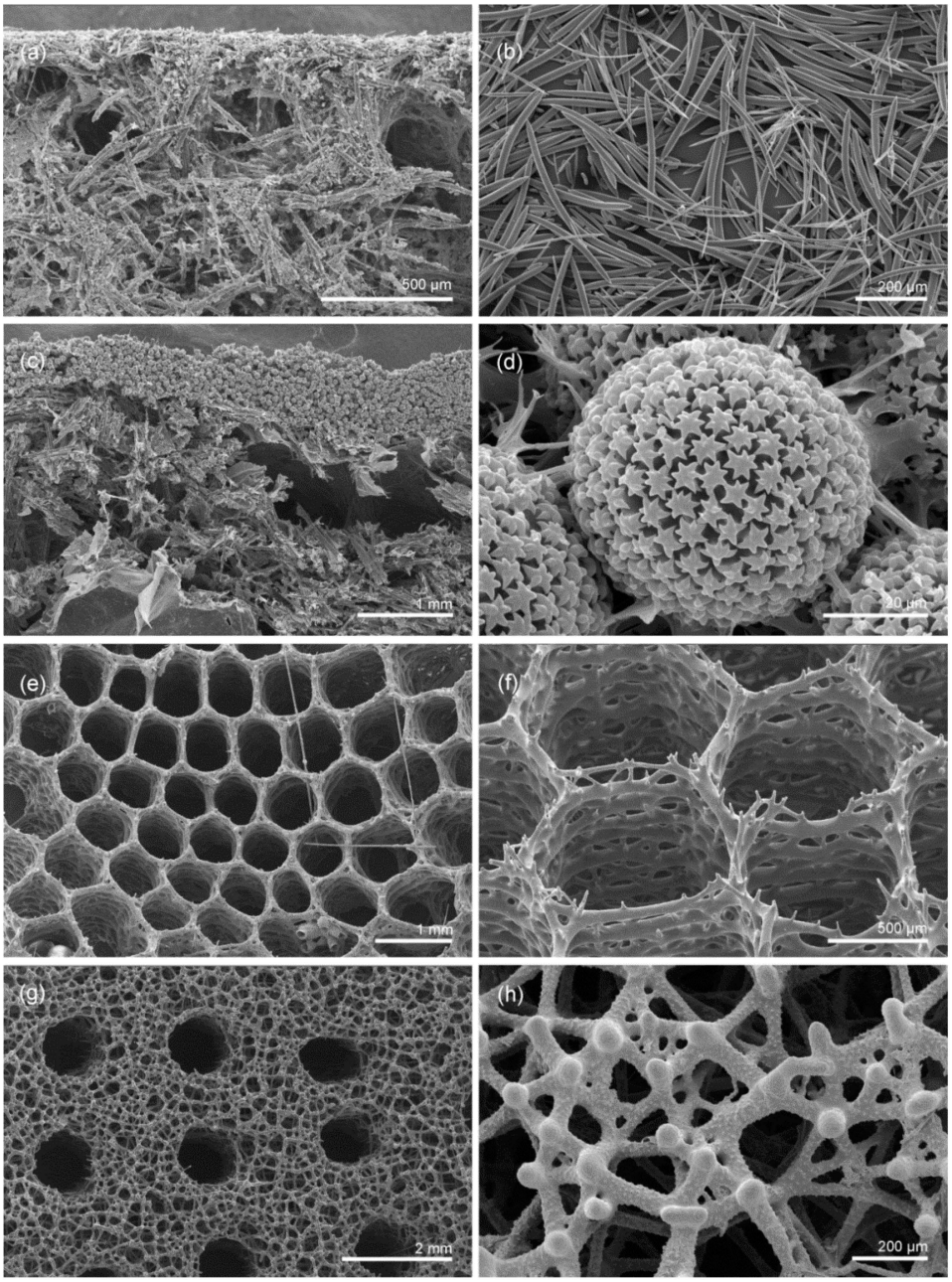

Figure 1. Scanning electron microscopy (SEM) images of the four samples investigated in this study. (**a**,**b**) Petrosid demosponge PETRO: (**a**) untreated, scale bar = 500 µm, (**b**) after organics removal, scale bar = 200 µm; (**c**,**d**) *Geodia* sp demosponge GEODIA: (**c**) untreated, scale bar = 1 mm, (**d**) untreated, scale bar = 20 µm; (**e**,**f**) *Aphrocallistes* sp. hexactinellid sponge APHRO: (**e**) untreated, scale bar = 1 mm, (**f**) after organics removal, scale bar = 500 µm; (**g**,**h**) *Laocoetis perion* hexactinellid LAOCO: (**g**) after organics removal, scale bar = 2 mm, (**h**) after organics removal, scale bar = 200 µm.

X-ray diffraction (XRD) patterns of the untreated samples showed broad peaks attributed to amorphous silica (Figure 2). GEODIA and LAOCO also showed the presence of quartz, PETRO, APHRO and LAOCO of calcium carbonates (calcite and/or aragonite) and PETRO and APHRO of halite, which are interpreted as foreign (detrital) grains and precipitate (halite) of sea water.

The results of Si, C, H, N and P elemental analyses are gathered in Table 1. All samples contain a large amount of Si, in the range 29%–35%, which is normal for such a siliceous sponge specimen, but cannot be used to discriminate them. PETRO and GEODIA have > 6% carbon content with

1.2%–1.5% N, suggesting that they contain a significant amount of organic matter, as expected for soft demosponges. In contrast, the C amount for APHRO and LAOCO is in the 2%–3% range, with a low N amount (<0.3%), suggesting that in hexactinellids the carbon is mainly related to carbonates, in agreement with the XRD data. A similar trend was observed for P content.

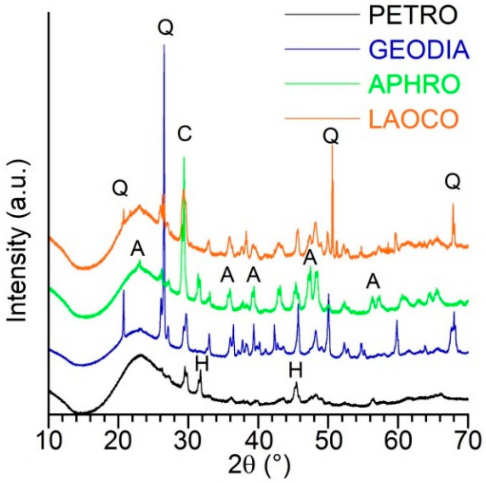

Figure 2. X-ray diffraction (XRD) patterns of the four samples. Main diffraction peaks were attributed to quartz (Q), calcite (C), aragonite (A) and halite (H).

Table 1. Si, C, H, N and P content (wt %) of the four samples as obtained by elemental analysis.

Sample	Si (wt %)	C (wt %)	H (wt %)	N (wt %)	P (wt %)
Petrosidae (PETRO)	33.99	6.60	1.61	1.55	0.11
Geodia (GEODIA)	28.76	6.81	1.39	1.23	0.18
Aphrocallistes (APHRO)	33.82	2.94	0.88	0.26	0.05
Laocoetis perion (LAOCO)	34.65	2.35	0.80	0.14	0.03

2.2. Solid State Nuclear Magnetic Resonance (NMR) Characterization

2.2.1. ^{29}Si Solid State NMR

The ^{29}Si NMR experiments were first carried out using the High Power Decoupling (HPDEC) Magic Angle Spinning (MAS) technique. These ^{29}Si HPDEC-MAS NMR experiments, which were undertaken under nearly quantitative conditions routinely well-adapted to amorphous silica gel-like material observation, as expected for such siliceous skeletons, all indicate that the silica network is well condensed. The ^{29}Si NMR spectra of the four samples (Figure 3) show three main broad lines attributed to Q_2, Q_3 and Q_4 species (*i.e.*, (SiO_4) units linked to two, three and four Si atoms, respectively), whose chemical shifts are respectively at *ca.* −92, −103 and −113 ppm. From spectral deconvolution, these three components are present in a typical proportion of 1%–2% (Q_2), 24%–26% (Q_3) and 73%–75% (Q_4) (Table 2), so that the final silica condensation degree D (*i.e.*, the ratio between Si–O–Si over Si–O–X (X = H, Si) bonds) is close to 0.93 for all samples.

There was no apparent difference between the classes or sampling/storage conditions of the samples, except the Q_4 narrow peak was pointed out as a shoulder at *ca.* −107 ppm on the ^{29}Si spectrum for GEODIA which is assignable to a crystalline polymorph such as quartz. It can be noticed that the real intensity of this component could have reached its theoretical maximum value if very long-running experiments, more applicable to particularly long spin-lattice relaxation times such as that of crystalline quartz, would have been carried out. A checking procedure, undertaken using intermediate acquisition conditions (300 s recycling delay at 30° pulse), indeed showed no significant enhancement in the intensity of this peak and no variation at all in the Q_2:Q_3:Q_4 ratio.

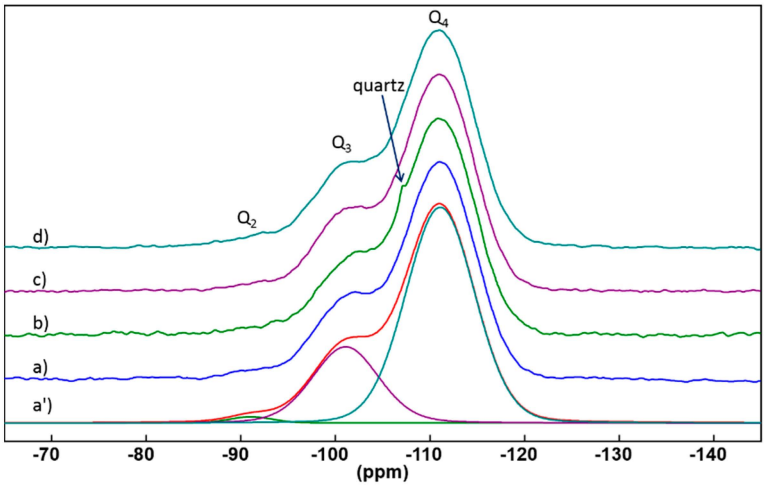

Figure 3. The ^{29}Si solid state nuclear magnetic resonance (NMR) spectra of the four samples (**a**) PETRO (number of scans = 1192); (**b**) GEODIA (number of scans = 960); (**c**) APHRO (number of scans = 1277) and (**d**) LAOCO (number of scans = 1080). For all spectra, the recycling delay was 60 s at 45° pulse. Figure 3**a′** shows the PETRO spectral deconvolution into Q_4, Q_3 and Q_2 contributions.

Table 2. Relative contribution of Q_2, Q_3 and Q_4 species to the ^{29}Si solid state nuclear magnetic resonance (NMR) spectra of the four samples as obtained from deconvolution.

Sample	Q_2 (%, ±1%)	Q_3 (%, ±1%)	Q_4 (%, ±1%)	D (±0.01)
Petrosidae (PETRO)	1	26	73	0.93
Geodia (GEODIA)	1	24	75	0.94
Aphrocallistes (APHRO)	1	26	73	0.93
Laocoetis perion (LAOCO)	2	25	73	0.93

2.2.2. ^{13}C Solid State NMR

The ^{13}C Cross-Polarization (CP)-MAS experiments were also carried out in order to identify the organic constituents of the samples (Figure 4). Only CP-MAS experiments were undertaken for ^{13}C MAS NMR to limit the acquisition time for each sample. In such conditions, only qualitative results can be obtained but the comparison of spectra acquired under the same conditions is perfectly allowed. The highest intensities are obtained with GEODIA and PETRO samples, *i.e.*, the soft demosponges. Spectra showed a good signal-to-noise ratio in agreement with the significant amount of C determined by chemical analysis. Their typical ^{13}C CP-MAS spectrum could be decomposed into different areas. The 0–80 ppm region is characterized by a broad band resulting from the overlap of numerous resonances that can be attributed to aliphatic C groups, such as –(CH_n)– fragments that could be found in proteins, polysaccharides or fatty acids (signal in the 0–40 ppm region), C–N bonds arising from protein chains (signal in the 40–60 ppm region) and C–O bonds likely due to carbohydrates (signal in the 60–80 ppm region). A very typical signal at 100–105 ppm can be noticed which is indicative for the C1 position in polysaccharides. The broad band at *ca.* 128 ppm corresponds to C=C double bonds of the fatty acid groups in phospholipids present in the cellular membranes and the signal at 157 ppm to C=N imine groups of amino acids. The sharp resonance at 174 ppm should correspond to amide or carbonyl groups that may be found in proteins or polysaccharides. We can also notice that no carbonate signal was detected (expected at 168.7 ppm for calcite and 171.0 ppm for aragonite [21]), although calcium carbonates were detected by XRD. This is very likely due to the fact that these non-hydrated phases are difficult to detect in such low-contact time Cross-Polarization conditions that favor the protein component against the carbonate one [22]. When the two samples are compared, one can notice that the relative intensity of the peaks at small chemical shifts can differ significantly,

suggesting the different composition of organic matter. In particular, the higher intensity of the peaks at 20 and 50 ppm for GEODIA would indicate a higher amount of carbohydrates compared to PETRO.

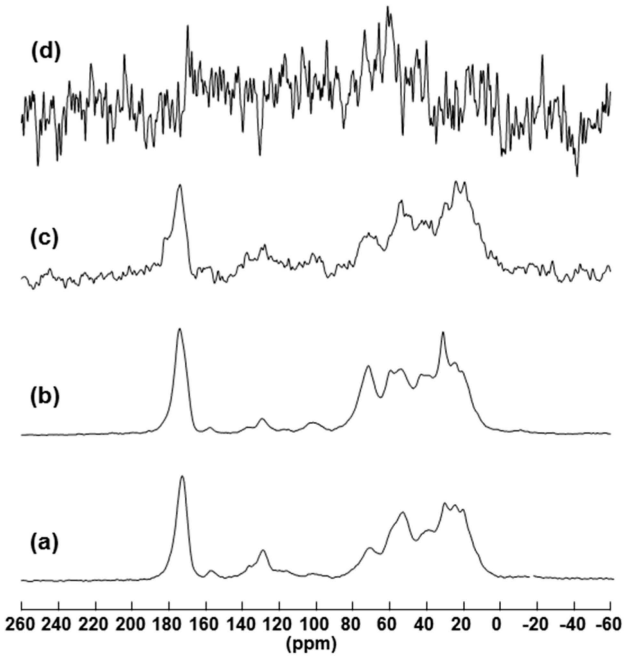

Figure 4. The ^{13}C Cross-Polarization (CP)-Magic Angle Spinning (MAS) NMR spectra of the four samples: (**a**) PETRO (number of scans = 79,200); (**b**) GEODIA (number of scans = 113,203); (**c**) APHRO (number of scans = 98,320); and (**d**) LAOCO (number of scans = 171,580). For all spectra, the ^{1}H–^{13}C contact time was 1 ms and the recycling delay was 2 s.

The hexactinellid APHRO spectrum showed a relatively poor signal-to-noise ratio, in agreement with a low C-content, but the main resonances were similar to the previous samples. However, an additional peak at 178 ppm is observed in addition to the peak at 174 ppm, which may correspond to carboxylate or amide functions of fatty acids or proteins, respectively. LAOCO, the other hexactinellid sample, gave almost no signal in the same acquisition conditions, in agreement with the low organic content indicated by elemental analysis. Remembering that LAOCO was collected dead and stored for a long time, it can be suggested that organic matter degradation has occurred. Interestingly, one should notice that the ^{29}Si signals were very similar for both APHRO and LAOCO, indicating that the sample evolution has only impacted its organic component, without significantly modifying the inorganic phase.

2.2.3. ^{31}P Solid State NMR

The ^{31}P HPDEC-MAS NMR spectra of the four samples are shown in Figure 5. For all samples, a broad signal centered at *ca.* 0 ppm is observed. This resonance can be considered as the sum of two contributions, the first one at −1.0 ppm for organic phosphates and the second one at +2.9 ppm for inorganic phosphates. The first signal was expected since sponges contain long-chain phospholipid fatty acids, with a large extent as long as 23–34 carbon atoms. The class of these phospholipids (PL), located mainly in the biological bilayer membrane, could vary a lot with sponge species, but phosphatidylethanolamine (PE) was found to usually be the major PL class in marine sponges, followed by phosphatidylcholine (PC) [23]. The second signal should correspond to remaining traces of intracellular phosphates. Depending on the sample, the balance between organic and inorganic phosphates could differ noticeably. Whereas GEODIA, APHRO and LAOCO contain a bigger proportion of inorganic phosphates, it is the reverse for PETRO which contains more organic ones.

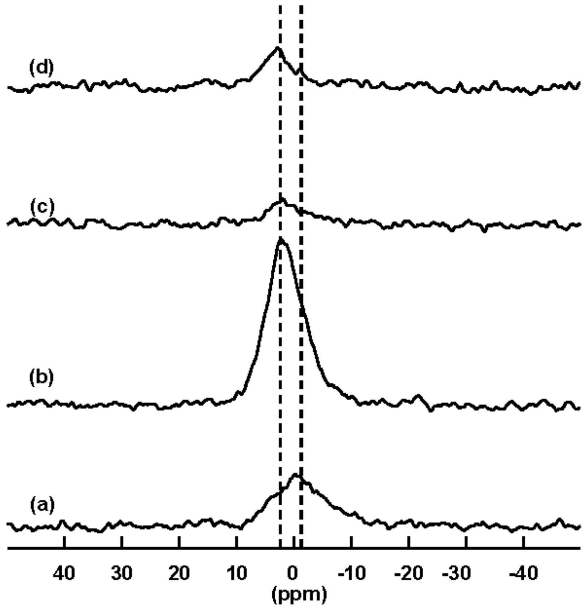

Figure 5. The ^{31}P High Power Decoupling-Magic Angle Spinning (HPDEC-MAS) NMR spectra of (**a**) PETRO; (**b**) GEODIA; (**c**) APHRO; and (**d**) LAOCO. For all spectra, the recycling delay was 10 s at 30° pulse and the number of scans was 600.

3. Discussion

In the case of silica-containing biological materials, previous studies have shown that the inorganic network was very similar regardless of the considered organism at a comparable state of diagenesis [16,18–20]. In particular, a previous ^{29}Si NMR study of diatoms [19] also showed that a condensation degree D of 0.93 (±0.01) was obtained. This is indicative of the fact that so-called biosilica is commonly built from silica nanoparticles so that its condensation degree is very similar to that of synthetic silica colloids. For instance, silica nanoparticles *ca.* 50 nm in size obtained by the Stöber process have a condensation degree of 0.93 (±0.01) [24], the same value as found here for the spicules. Considering the organic matter, desmosponges and hexactinellids cannot be easily distinguished from its composition, as obtained by ^{13}C NMR, but rather by its abundancy. Altogether, this suggests that despite the fact that they belong to different groups of the phylum Porifera with strikingly different morphologies, these sponges cannot be differentiated through simple NMR analyses. It would therefore be necessary to perform additional treatments to the spicules, such as demineralization or extraction procedures, to get access to organic fractions that may allow for the differentiation of groups. In parallel, NMR analyses of whole samples can distinguish samples on the basis of their sampling conditions, especially via organic matter degradation, a point of interest for further research.

4. Materials and Methods

4.1. Main Techniques of Characterization

The microstructure of the material was investigated by SEM using a Philips XL20 microscope (Philips, Eindhoven, The Netherlands). For organics removal, a standard procedure, previously described [19], was undertaken, which consists in boiling the samples in HNO_3 to ensure complete organic matter degradation, then rinsing them several times with distilled water and finally drying them with propanol. The crystalline phases of the raw material were then identified using a powder X-ray diffractometer (XRD) Bruker D8 Advance (Bruker AXS, GmbH, Karlsruhe, Germany). The diffractograms were collected ranging from 5° to 70° using a 0.01°/s step size and the CuKα radiation. The sample powder was chemically analyzed by inductively coupled plasma atomic

emission spectrometry (ICP-AES), carried out at the Service Central d'Analyse, CNRS, Solaize, France, that is an analytical technique routinely used for the detection of trace elements.

4.2. Solid State NMR Studies

The ^{29}Si, ^{13}C and ^{31}P solid state NMR experiments were performed on an Avance III 300 Bruker spectrometer (7.04 Tesla static magnetic field) equipped with Bruker 4BL and 7BL CP/MAS 1H/BB probes (Bruker BioSpin, GmbH, Karlsruhe, Germany). Raw samples were ground and packed into ZrO_2 rotors (4 and 7 mm diameter, respectively) before spinning at 14 or 5 kHz, respectively. Magic Angle Spinning (MAS) and High Power Decoupling (HPDEC [25], spinal 64, ν_{1H} = 50 kHz) were used during acquisition both for single pulse (HPDEC-MAS) experiments, which are quantitative, and Cross Polarization (CP-MAS) experiments, which are not. The Free Induction Decay (FID) data were processed using Topspin software (Bruker BioSpin) and a line broadening (LB) was applied before Fourier transformation. All chemical shifts (δ) were referenced to tetramethylsilane (TMS; δ = 0 ppm).

The {^{1}H}-^{13}C CP-MAS NMR experiments were carried out at a frequency of 75.51 MHz, using 2 s recycling delay at 90° pulse and 1 ms contact time, collecting until *ca.* 170,000 transients (number of scans, NS) in case of poor carbon content. CP-MAS technique is routinely used in solid state NMR for non-abundant nuclei signal enhancement, even if this method is not quantitative. The concept lies on a magnetization transfer from ^{1}H abundant nuclei to less abundant ^{13}C ones. Taking into account that ^{13}C natural abundance is only 1.1%, it allows to get realistic the acquisition of spectra from C-poor content samples with a reasonable signal/noise ratio. Despite the non-quantitativity of the method, the comparison of CP spectra of samples within the same series is relevant if they are recorded in the same conditions.

The ^{29}Si HPDEC-MAS NMR experiments were carried out at a frequency of 59.66 MHz, using 60 s recycling delay at 45° pulse, conditions that allow to be respectful to the relaxation of the ^{29}Si nuclei in the silica gel and to provide quantitative results. Spectra were processed using DmFit modeling software [26] leading to the various Q_n (n = 0 to 4, integer) percentages obtained for the spectral components. A condensation degree D of the silica network can then be defined as

$$D = \frac{\sum_{n=0}^{4} nQ_n}{4\sum_{n=0}^{4} Q_n}$$

which represents the number of effective Si–O–Si linkages among all the theoretical possibilities of connectivity.

The ^{31}P HPDEC-MAS NMR experiments were carried out at 121.56 MHz, using 10 s recycling delay at 30° pulse and NS = 600. Complete relaxation was checked with longer recycling delays, showing no signal increase and thus enabling to get quantitative results.

5. Conclusions

Despite the fact that typical morphologies were observed by SEM for each sample, no significant difference was firstly observed by ^{29}Si HPDEC-MAS NMR. A more detailed analysis, conducted especially by ^{13}C CP-MAS and ^{31}P HPDEC-MAS.

NMR, showed that the sampling and storage conditions of the specimens had a great impact on the results, depending mainly on the degree of organic matter degradation. Further investigations, involving a larger collection of sponges, as well as complementary methods of characterization, have to be considered to improve the understanding of such natural complex systems.

Acknowledgments: This study has been supported by statuary funds of the Institute of Paleobiology to Andrzej Pisera. This work was supported by FRENCH state funds managed by the ANR within the Investissements d'Avenir programme under reference ANR-11-IDEX-0004-02, and more specifically within

the framework of the Cluster of Excellence MATISSE (MATériaux, Interfaces, Surfaces, Environment) led by Sorbonne Universités.

Author Contributions: Sylvie Masse, Andrzej Pisera and Thibaud Coradin conceived and designed the experiments; Sylvie Masse, Andrzej Pisera and Guillaume Laurent performed the experiments; Sylvie Masse, Andrzej Pisera, Guillaume Laurent and Thibaud Coradin analyzed the data and wrote the paper.

Conflicts of Interest: The authors declare no conflict of interest.

References

1. Mann, S. Molecular tectonics in biomineralization and biomimetic materials chemistry. *Nature* **1993**, *365*, 499–505. [CrossRef]
2. Coradin, T.; Lopez, P.J.; Gautier, C.; Livage, J. From biogenic to biomimetic silica. *C. R. Palevol* **2004**, *3*, 443–452. [CrossRef]
3. Patwardhan, S.V. Biomimetic and bioinspired silica: Recent developments and applications. *Chem. Commun.* **2011**, *47*, 7567–7582. [CrossRef] [PubMed]
4. Ragueneau, O.; Tréguer, P.; Leynaert, A.; Anderson, R.F.; Brzezinski, M.A.; DeMaster, D.J.; Dugdale, R.C.; Dymond, J.; Fischer, G.; François, R.; *et al*. A review of the Si cycle in the modern ocean: Recent progress and missing gaps in the application of biogenic opal as a paleoproductivity proxy. *Glob. Planet Chang.* **2000**, *26*, 317–365. [CrossRef]
5. Boury-Esnault, N. Le rôle de la silice dans la biosphère: L'exemple des spongiaires. *C. R. Chim.* **2008**, *11*, 261–267. (In French) [CrossRef]
6. Hooper, N.A.V.; Soest, R.W.M. (Eds.) *Systema Porifera: A Guide to the Classification of Sponges*; Kluwer Academic Publishers: New York, NY, USA, 2002.
7. Pisera, A. Some aspects of silica deposition in lithistid demosponge desmas. *Microsc. Res. Tech.* **2003**, *62*, 312–326. [CrossRef] [PubMed]
8. Shimizu, K.; Cha, J.; Stucky, G.D.; Morse, D.E. Silicatein alpha: Cathepsin L-like protein in sponge biosilica. *Proc. Natl. Acad. Sci. USA* **1998**, *95*, 6234–6238. [CrossRef] [PubMed]
9. Müller, W.E.G.; Wang, X.; Kropf, K.; Ushijima, H.; Geurtsen, W.; Eckert, C.; Nawaz Tahir, M.; Tremel, W.; Boreiko, A.; Schlossmacher, U.; *et al*. Bioorganic/inorganic hybrid composition of sponge spicules: Matrix of the giant spicules and of the comitalia of the deep sea hexactinellid Monorhaphis. *J. Struct. Biol.* **2008**, *161*, 188–203. [CrossRef] [PubMed]
10. Sumper, M.; Brunner, E. Learning from diatoms: Nature's tools for the production of nanostructured silica. *Adv. Funct. Mater.* **2006**, *16*, 17–26. [CrossRef]
11. Wang, X.; Schröder, H.C.; Wang, K.; Kaandorp, J.A.; Müller, W.E.G. Genetic, biological and structural hierarchies during sponge spicule formation: From soft sol-gels to solid 3D silica composite structures. *Soft Mater.* **2012**, *8*, 9501–9518. [CrossRef]
12. Coradin, T.; Lopez, P.J. Biogenic silica patterning: Simple chemistry or subtle biology? *Chembiochem* **2003**, *4*, 251–259. [CrossRef] [PubMed]
13. Mann, S.; Perry, C.C.; Williams, R.J.P.; Fyfe, C.A.; Gobbi, G.C.; Kennedy, G.J. The characterization of the nature of silica in biological systems. *J. Chem. Soc. Chem. Commun.* **1983**, *4*, 168–170. [CrossRef]
14. Gendron-Badou, A.; Coradin, T.; Maquet, J.; Frohlich, F.; Livage, J. Spectroscopic characterization of biogenic silica. *J. Non Cryst. Solids* **2003**, *316*, 331–337. [CrossRef]
15. Abramson, L.; Wirick, S.; Lee, C.; Jacobsen, C.; Brandes, J.A. The use of soft X-ray spectromicroscopy to investigate the distribution and composition of organic matter in a diatom frustule and a biomimetic analog. *Deep Sea Res. II* **2009**, *56*, 1369–1380. [CrossRef]
16. Sandford, F. Physical and chemical analysis of the siliceous skeletons in six sponges of two groups (Demospongiae and Hexactinellida). *Microsc. Res. Tech.* **2003**, *62*, 336–355. [CrossRef] [PubMed]
17. Bonhomme, C.; Coelho, C.; Baccile, N.; Gervais, C.; Azaïs, T.; Babonneau, F. Advanced solid state NMR techniques for the characterization of sol–gel-derived materials. *Acc. Chem. Res.* **2007**, *40*, 738–746. [CrossRef] [PubMed]
18. Bertermann, R.; Kröger, N.; Tacke, R. Solid-state ^{29}Si MAS NMR studies of diatoms: Structural characterization of biosilica deposits. *Anal. Bioanal. Chem.* **2003**, *375*, 630–634. [PubMed]

19. Tesson, B.; Masse, S.; Laurent, G.; Maquet, J.; Livage, J.; Martin-Jezequel, V.; Coradin, T. Contribution of multi-nuclear solid state NMR to the characterization of the Thalassiosira pseudonana diatom cell wall. *Anal. Bioanal. Chem.* **2008**, *390*, 1889–1898. [CrossRef] [PubMed]
20. Beterman, R.; Tacke, R. Solid-state ^{29}Si VACP/MAS NMR studies of silicon-accumulating plants: Structural characterization of biosilica deposits. *Ziet. Naturforsch. B* **2000**, *55*, 459–461.
21. Michel, F.M.; MacDonald, J.; Feng, J.; Phillips, B.L.; Ehm, L.; Tarabrella, C.; Parise, J.B.; Reeder, R.J. Structural characteristics of synthetic amorphous calcium carbonate. *Chem. Mater.* **2008**, *20*, 4720–4728. [CrossRef]
22. Nassif, N.; Pinna, N.; Gehrke, N.; Antonietti, M.; Jäger, C.; Cölfen, H. Amorphous layer around aragonite platelets in nacre. *PNAS* **2005**, *102*, 12653–12655. [CrossRef] [PubMed]
23. Genin, E.; Wielgosz-Collin, G.; Njinkoué, J.M.; Velosaotsy, N.E.; Kornprobst, J.M.; Gouygou, J.P.; Vacelet, J.; Barnathan, G. New trends in phospholipid class composition of marine sponges. *Comp. Biochem. Physiol. B Biochem. Mol. Biol.* **2008**, *150*, 427–431. [CrossRef] [PubMed]
24. Masse, S.; Laurent, G.; Chuburu, F.; Cadiou, C.; Deschamps, I.; Coradin, T. Modification of the stöber process by a polyazamacrocycle leading to unusual core-shell silica nanoparticles. *Langmuir* **2008**, *24*, 4026–4031. [CrossRef] [PubMed]
25. Fung, B.M.; Khitrin, A.K.; Ermolaev, K. An improved broadband decoupling sequence for liquid crystals and solids. *J. Magn. Reson.* **2000**, *42*, 97–101. [CrossRef] [PubMed]
26. Massiot, D.; Fayon, F.; Capron, M.; King, I.; Le Calvé, S.; Alonso, B.; Durand, J.O.; Bujoli, B.; Gan, Z.; Hoatson, G. Modelling one- and two-dimensional solid-state NMR spectra. *Magn. Reson. Chem.* **2002**, *40*, 70–76. [CrossRef]